



---

**Integration of Peptides into Organic Thin Film Transistor (OTFT)-based Printable Sensors**

**Paul Dastoor**

**UNIVERSITY OF NEWCASTLE RESEARCH SERVICES GRANTS OFFICE**

---

**02/10/2017**

**Final Report**

**DISTRIBUTION A: Distribution approved for public release.**

**Air Force Research Laboratory  
AF Office Of Scientific Research (AFOSR)/ IOA  
Arlington, Virginia 22203  
Air Force Materiel Command**

<b>REPORT DOCUMENTATION PAGE</b>				Form Approved OMB No. 0704-0188	
<p>The public reporting burden for this collection of information is estimated to average 1 hour per response, including the time for reviewing instructions, searching existing data sources, gathering and maintaining the data needed, and completing and reviewing the collection of information. Send comments regarding this burden estimate or any other aspect of this collection of information, including suggestions for reducing the burden, to Department of Defense, Executive Services, Directorate (0704-0188). Respondents should be aware that notwithstanding any other provision of law, no person shall be subject to any penalty for failing to comply with a collection of information if it does not display a currently valid OMB control number.</p> <p>PLEASE DO NOT RETURN YOUR FORM TO THE ABOVE ORGANIZATION.</p>					
<b>1. REPORT DATE (DD-MM-YYYY)</b> 13-02-2017		<b>2. REPORT TYPE</b> Final		<b>3. DATES COVERED (From - To)</b> 22 Apr 2015 to 21 Oct 2016	
<b>4. TITLE AND SUBTITLE</b> Integration of Peptides into Organic Thin Film Transistor (OTFT)-based Printable Sensors				<b>5a. CONTRACT NUMBER</b>	
				<b>5b. GRANT NUMBER</b> FA2386-15-1-4002	
				<b>5c. PROGRAM ELEMENT NUMBER</b> 61102F	
<b>6. AUTHOR(S)</b> Paul Dastoor				<b>5d. PROJECT NUMBER</b>	
				<b>5e. TASK NUMBER</b>	
				<b>5f. WORK UNIT NUMBER</b>	
<b>7. PERFORMING ORGANIZATION NAME(S) AND ADDRESS(ES)</b> UNIVERSITY OF NEWCASTLE RESEARCH SERVICES GRANTS OFFICE UNIVERSITY DRIVE CALLAGHAN, 2289 AU				<b>8. PERFORMING ORGANIZATION REPORT NUMBER</b>	
<b>9. SPONSORING/MONITORING AGENCY NAME(S) AND ADDRESS(ES)</b> AOARD UNIT 45002 APO AP 96338-5002				<b>10. SPONSOR/MONITOR'S ACRONYM(S)</b> AFRL/AFOSR IOA	
				<b>11. SPONSOR/MONITOR'S REPORT NUMBER(S)</b> AFRL-AFOSR-JP-TR-2017-0009	
<b>12. DISTRIBUTION/AVAILABILITY STATEMENT</b> A DISTRIBUTION UNLIMITED: PB Public Release					
<b>13. SUPPLEMENTARY NOTES</b>					
<b>14. ABSTRACT</b> <p>Biosensors based on organic thin film transistor technology offer the exciting prospect of detecting and identifying peptides; biomarkers found in bodily fluids. This development would assist in the monitoring or identification of medical diseases and facilitate rapid, point-of-care testing. In particular, neuropeptide Y is a highly abundant neurotransmitter with links to many important physiological functions, including stress response. Its rapid detection provides an opportunity to identify anxiety and stress related disorders such as post-traumatic stress disorder. Moreover, inkjet printing of organic electronic inks may provide a pathway for reliable, large scale production of low cost sensors. In this project, multiple detection mechanisms for two different peptides, L-reduced glutathione and neuropeptide Y, are presented. A pathway for impedance-based peptide detection using Nafion films was also presented. Receptor elements for glutathione detection were incorporated into the sensor device structure and a current response three times larger than that of water was obtained when 2 mM glutathione was placed on the sensor. This response demonstrated an increase in sensitivity of five times over the non-transistor based sensing mechanism. Electrochemical detection of neuropeptide Y was also achieved, with the method proposed, utilising monoclonal anti-neuropeptide Y antibodies, enabling detection of neuropeptide Y concentrations below 95 nM.</p>					
<b>15. SUBJECT TERMS</b> <p>organic thin film transistors, AOARD, printable sensors</p>					
<b>16. SECURITY CLASSIFICATION OF:</b>			<b>17. LIMITATION OF ABSTRACT</b>  SAR	<b>18. NUMBER OF PAGES</b> 15	<b>19a. NAME OF RESPONSIBLE PERSON</b> CASTER, KENNETH
<b>a. REPORT</b>  Unclassified	<b>b. ABSTRACT</b>  Unclassified	<b>c. THIS PAGE</b>  Unclassified			<b>19b. TELEPHONE NUMBER (Include area code)</b> 315-229-3326

## Integration of Peptides into OTFT-based Printable Sensors

Dec 12, 2016

**Name of Principal Investigators:** Paul C Dastoor, Warwick J Belcher, Xiaojing Zhou

- e-mail address: Paul.Dastoor@newcastle.edu.au
- Institution: University of Newcastle
- Mailing Address: Centre for Organic Electronics, University of Newcastle, Callaghan, NSW 2308, Australia.
- Phone: +61-2-49215426

Period of Performance: 22/04/2015 – 21/10/2016

**Abstract:** Biosensors based on organic thin film transistor technology offer the exciting prospect of detecting and identifying peptides; biomarkers found in bodily fluids. This development would assist in the monitoring or identification of medical diseases and facilitate rapid, point-of-care testing. In particular, neuropeptide Y is a highly abundant neurotransmitter with links to many important physiological functions, including stress response. Its rapid detection provides an opportunity to identify anxiety and stress related disorders such as post-traumatic stress disorder. Moreover, inkjet printing of organic electronic inks may provide a pathway for reliable, large scale production of low cost sensors. In this project, multiple detection mechanisms for two different peptides, L-reduced glutathione and neuropeptide Y, are presented. A pathway for impedance-based peptide detection using Nafion films was also presented. Receptor elements for glutathione detection were incorporated into the sensor device structure and a current response three times larger than that of water was obtained when 2 mM glutathione was placed on the sensor. This response demonstrated an increase in sensitivity of five times over the non-transistor based sensing mechanism. Electrochemical detection of neuropeptide Y was also achieved, with the method proposed, utilising monoclonal anti-neuropeptide Y antibodies, enabling detection of neuropeptide Y concentrations below 95 nM.

**Introduction:** Organic electronics is a field that has attracted significant interest over the past few decades as there has been steady improvement in the electrical performance and stability of these organic electronic devices [1]. Organic electronic materials are inexpensive compared to conventional silicon devices due to their ability to be manufactured at large scale using low-cost printing techniques; providing a further driver for their implementation to a number of technological areas. Their ability to be solution processed is highly advantageous, allowing many different highly cost effective fabrication techniques to be used such as drop casting [2], spin coating [3] and inkjet printing [4].

Inkjet printing is an additive process in which the patterning and the material deposition occur at the same time [3]. After the required pattern has been digitally developed, the printer deposits the material exactly where required, providing consistency to the process and enabling a large number of devices to be produced simultaneously, reducing production time. This process also enables the devices to be printed directly onto flexible substrates as these materials do not require high temperature exposure (>150 °C) during the fabrication process so that the plastic films maintain their structural integrity.

The low voltage operation of these sensors ensures low power consumption and minimal electrochemical damage to the sensing material [3]. In addition, for aqueous based media, these low operating voltages allow device operation to be maintained within the water window (1.23 V) thus preventing device failure due to electrochemical water splitting [5]. Recent work in this laboratory has shown that glucose enzymes (proteins) are able to be integrated into organic thin film transistor (OTFT) sensors [2]; highlighting that it is possible to integrate peptides (linked short chains of amino acid monomers) or anti-peptide antibodies into organic electronic devices more easily than into conventional

inorganic sensors.

A peptide is a short chain amino acid monomer that is linked by a covalent peptide bond, also known as an amide bond [6]. An amino acid is an organic compound that contains carboxylic acid (-COOH) and amine (-NH<sub>2</sub>) functional groups [7]. Peptides can become quite large and complex and are described as a protein when their amino acid count rises above approximately 50 monomers [8,9]. Peptides are found in every cell and tissue in humans and perform a wide range of functions that are essential in maintaining good health. Functions depend on the types of amino acids in the chain as well as the sequence and shape of the peptide [9].

Peptide and protein identification is crucial in the study of disease, related biomarkers, and specific metabolic activity [10]. Currently, peptides are detected using a combination of high performance liquid chromatography (HPLC) and targeted mass spectrometry [10-15]. However, these tests require extensive equipment and are complex measurements. Peptide detection is also possible using fluorescence resonance energy transfer (FRET), whereby a sensor molecule is introduced, which produces an increase in the fluorescence of the system upon binding with the peptide [16]. FRET-based biosensors have been successfully developed [17-19] with imaging in live cells possible [20]. Through the observation of the emission spectrum of peptides that contain known residues, it is also possible to identify peptides or proteins [8-21]. It is common to use either fluorescent or radioactive labelling to identify peptides as they allow for the investigation of interactions such as binding or enzyme activity [22]. Western blot analytical techniques are used in which the proteins are separated based on their size, using gel electrophoresis, and then transferred to a membrane that is covered with protein specific labelled antibodies, allowing them to be visibly identified after developing the membrane [23]. Also, enzyme-linked immunosorbent assays (ELISA) can be performed to detect antigens, peptides, and proteins through a colour change after an enzyme linked antibody binds to its substrate [24].

Although the aforementioned detection mechanisms are useful, they are all inherently indirect since the detection process requires an intermediate step to convert the signal (whether optical or otherwise) into an electronic voltage. Electrochemical detection mechanisms are of much greater interest as these enable a direct electrical response to be observed and electronically amplified for detection. Electrochemical methods have been used to detect peptides through the oxidation of Cu(II)-peptide complexes via the corresponding Cu(III) complexes [25,26]. Alternatively, some peptides can have their surface amino acid residues electrochemically oxidised and this response measured [27]. It has also been shown that it is possible to oxidise and cleave proteins electrochemically and then detect the resulting peptides using mass spectrometry [28].

Glutathione (GSH) is a tripeptide with chemical formula C<sub>10</sub>H<sub>16</sub>N<sub>3</sub>O<sub>6</sub>SH as shown in Figure 1. It is a key reactant of intercellular metabolic processes and the ratio of reduced glutathione to oxidised glutathione in cells can be used as a measure of oxidative stress [29]. Oxidative stress is a measure of how imbalanced the redox state of cells are, and is thought to have a part in the development of a number of diseases including Asperger syndrome [30], attention deficit hyperactivity disorder (ADHD) [31], cancers [32], and Alzheimer's disease [33]. This peptide was also chosen as thiol groups are known to bind to gold surfaces with high affinity through the formation of Au-sulfur bonds [34]. This high affinity allows for a self-assembled monolayer (SAM) to be formed which alters the impedance of the electrode as it forms an insulating layer on its surface which depends on the degree of coverage and quality, such as the occurrence of pin-holes [35].

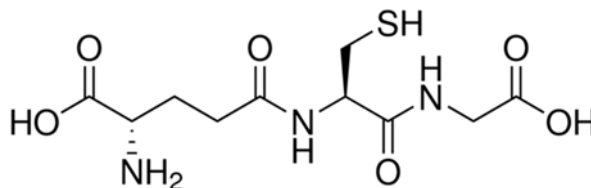


Figure 1: Chemical structure of Glutathione (GSH)

Glutathione S-Transferases (GSTs) are a family of enzymes that catalyse the conjugation of reduced glutathione to foreign chemical substances [36,37] and can also bind to GSH [38]. As this is a bio-specific interaction, the selectivity of this type of sensing mechanism is good. The structure of GST is shown in Figure 2.

It is believed that holes, in a GSH SAM prepared on a gold electrode, occur when it is exposed to substances such as transition metal ions, rare earth metals, or neurotransmitters. These holes occur because they change the shape of GSH from a T shape to a Y shape through interactions with specific functional groups [39,40]. As the same functional group of GSH is important when interacting with GST, the change in the shape of the GSH SAM can also occur. Therefore, it is thought that GST modifies the GSH layer, which leads to pinholes being created on the surface. As the SAM is not as insulating, this results in charge transfer with the ferricyanide being enhanced [41].

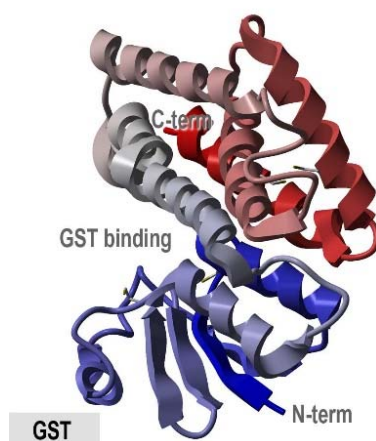


Figure 2 Crystallographic structure of the glutathione S-transferase (GST) enzyme

NPY is a peptide comprising of 36 amino acids that acts as a neurotransmitter through the central and peripheral nervous systems. It has roles in many diverse bodily processes such as the regulation of food intake, stress, pain, blood pressure, and hormone secretion, as well as having links with a number of diseases such as depression and anxiety [42, 43]. It has a tertiary structure shown in Figure 3 and chemical formula of  $C_{190}H_{287}N_{55}O_{57}$ , with slight variations depending on how it is produced. For example, the human NPY used in the following experiments has chemical formula  $C_{189}H_{285}N_{55}O_{57}S$  and a molecular weight of 4271.68 g/mol and over 95% purity [44].

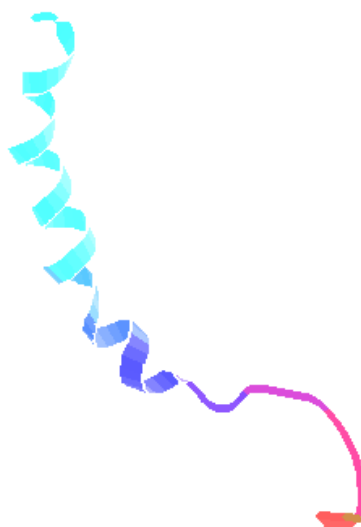


Figure 3: Nuclear magnetic resonance spectroscopy image of NPY structure [45]

The receptor for the NPY antigen is the Anti-NPY antibody. Antibodies, also known as immunoglobulins, are produced by B lymphocytes and secreted into plasma [46]. They are Y shaped proteins that highly selectively bind to antigens, with an interaction synonymous with a lock and key mechanism. The tip of each Y branch contains a paratope that is specific for a particular epitope on an antigen. The basic structure of an antibody is shown in Figure 4 indicating that each antibody monomer is able to bind with two antigen molecules. There are also subclasses of immunoglobulin including IgA, IgD, IgE, IgG, and IgM which correspond to different heavy chain regions. The anti-NPY used is an isotope IgG1 $\kappa$  which is in the IgG class, heavy chain subclass 1, and has  $\kappa$  type light chains. In humans,  $\kappa$  chains are found 67 % of the time and  $\lambda$  chains are found 33 % of the time [46]. Anti-NPY was selected due to its high selectivity to NPY, specifically, NPY in humans. Also, the anti-NPY selected is monoclonal and has a specific affinity to human NPY. Therefore, it will not bind to sheep, rat, or porcine NPY and this ensures that any systems investigated with have extremely high selectivity.

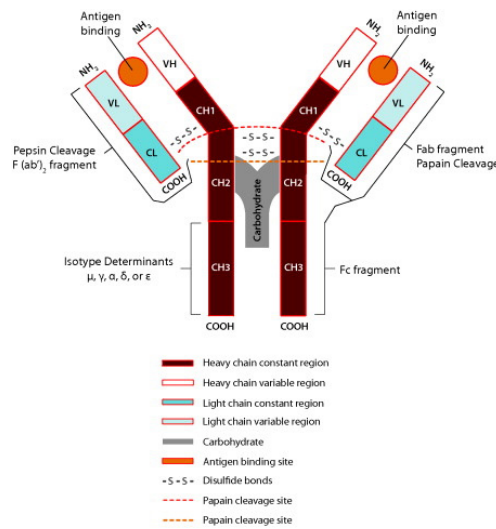


Figure 4: Basic antibody structure [46].

There are two major neuropeptides that are able to assist in the diagnosing of stress, depression, anxiety and trauma, NPY and Orexin A (OXA) [42,47]. Hagen et al. [48] developed a zinc oxide field effect transistor (FET) that could detect OXA down to a picomolar concentration in water. They used multiple binding peptides with varying affinities, attached to the ZnO surface using a residue linker, that enabled preferential binding to the semiconductor over any other surface. This surface of the FET was then exposed to varying concentrations of OXA. As OXA has an overall positive charge, the current increased with an increase in OXA concentration, with it beginning to saturate at higher concentration as the number of available binding sites was reducing.

Sanghavi et al. [49] presented an alternative sensing mechanism for both NPY and OXA. They used high frequency electrokinetic pre-concentration of the peptides into a nanochannel to enable the detection of these neuropeptides at picomolar concentrations. This dielectrophoresis ensures that the NPY molecules are trapped in the nanochannel and smaller molecules such as dopamine are only able to get to the electrode by free diffusion, thereby reducing interference. By using a microfluidic device they are able to detect the oxidation of NPY or OXA on the high conductivity graphene modified electrodes.

In this project, detection of two peptides (GSH and NPY) using an OTFT structure has been investigated. In both cases, the GSH-GST linkage has been exploited to enable binding to the peptide unit. By integrating the linking moiety into the Nafion gate electrode, selective binding of either GSH or NPY can be achieved.

## Experiment:

### OTFT Fabrication

ITO patterned glass slides purchased from Xinyan Technology Ltd. were ultrasonically cleaned

(Branson 2510 Ultrasonic Cleaner) in a 1 % Micro-90 concentrated cleaning solution in Milli-Q water for 30 minutes. The substrates were then thoroughly rinsed with Milli-Q water to remove the surfactant and then rinsed with isopropanol. They were then rinsed with Milli-Q water again and blown dry using a nitrogen gun. The substrates are then placed in a Bioforce Nanosciences UV-ozone ProCleaner for 15 minutes. The P3HT layer was spin coated from a 20mg/ml solution in chloroform and then heated on a hotplate at 45 °C until the solvent was fully evaporated. The PVP layer was spin coated from a 80mg/ml solution in ethanol and then heated on a hotplate at 80 °C for 10 minutes. Nafion was spin coated onto the ITO patterned substrates at 500 rpm for two minutes, giving a thickness of approximately 350 nm.

#### Device Testing

Two Keithley 2400 SourceMeters were used, which communicate to a computer through LabView software. These devices allow for  $V_{DS}$  and  $V_{GS}$  to be fixed while also measuring the currents  $I_D$  and  $I_G$ . Therefore, it is possible to obtain both the output characteristic and the transfer curve for the devices. Sensor measurements were also taken in which  $I_D$  and  $I_G$  were measured as a function of time with fixed  $V_{DS}$  and  $V_{GS}$ . Cyclic voltammetry was achieved using a Obbligate Objectives Faraday MP Scanning Potentiostat Model F02A and was calibrated using the ferricyanide-ferrocyanide couple.

#### Results and Discussion:

The time dependence of the electrochemical detection of the GSH tripeptide was determined using sensor films consisting of GST embedded into a commercial polyelectrolyte membrane (Nafion). Two different films were prepared: (1) 1  $\mu$ M GST in Nafion spin coated onto a conductive indium tin oxide (ITO) substrate and (2) a control Nafion film spun onto an ITO substrate. The voltage across the electrodes was set to 1 V and after 200 seconds, a drop of either GSH or buffer solution was placed on the device. The results from these tests are shown in Figure 5. It is noted that representative curves are shown, indicative standard deviation error bars are placed on the end of each curve, and that current was normalised to this initial value immediately prior to droplet application ( $t=190$  s) to account for any differences in initial conductivity of the Nafion film before the drop was placed onto the device. It can be seen that when there was no GST incorporated into the film, the response of the buffer solution and the GSH appeared to be similar. There was an exponential decrease in current when the voltage was set across the device, after which it began to stabilise. This was followed by analyte drop, which caused the current to significantly increase for a very short amount of time as this drop disrupted the current pathways within the film. After approximately 200 seconds, the current returned to its original value, before the analyte was placed on the film. This return to the same relative current value was independent of whether GSH or buffer was dropped on the film. However, it can be seen that there was a significant difference in the final current between the GSH and buffer devices (Figure 5B). This difference indicates that there is a significant interaction between the GST and GSH that modifies the current pathways through the film and reduces the final impedance of the device.

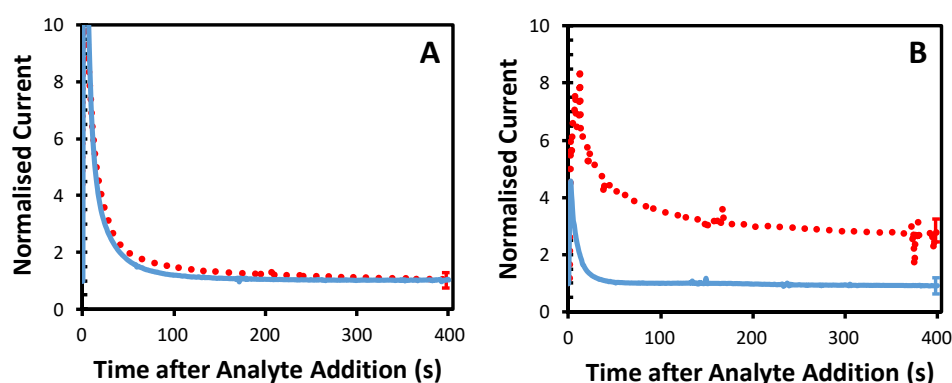


Figure 5: Peptide sensor response to buffer solution (solid blue line) and GSH peptide solution (red dotted line) for a control Nafion film (A) and a film consisting of GST embedded in Nafion (B). Error bars show the standard deviation of the measurement.

The data shown in Figure 5 indicates that peptide detection is possible using the change in impedance of the GST embedded Nafion membrane. Previous work in this laboratory has shown that it is possible to obtain an amplified glucose detection using a Nafion film embedded with glucose oxidase (GOX)



enzyme as part of the gate in an OTFT structure [50]. In this device architecture (Figure 6), protons generated by the GOX enzyme action on glucose at the gate diffuse through the device to the semiconducting polymer (poly 3-hexylthiophene (P3HT)) interface whereupon the conductivity of the channel is altered. Thus, while impedance-based peptide detection is an important step in demonstrating that the GSH-GST binding process is working, impedance based detection alone is insufficient for integration into our OTFT architecture. In particular, we need to have a mechanism that allows for the generation of protons following peptide detection at the gate electrode.

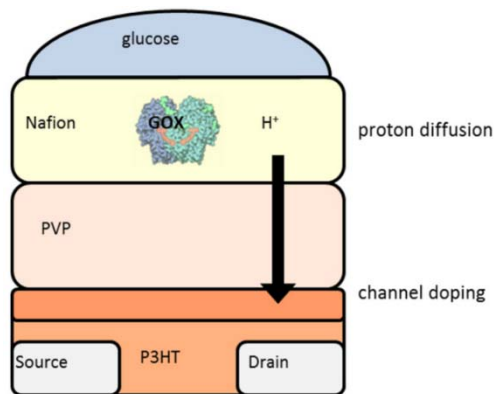
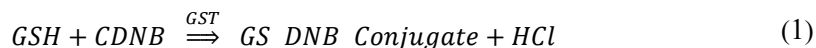


Figure 6: Operation and structure of enzyme-based glucose sensors developed at the Centre of Organic Electronics (COE), University of Newcastle [50]. The glucose oxidase (GOX) enzyme is embedded in the Nafion film and detection occurs via the generation of protons ( $H^+$ ) that subsequently diffuse across the polyvinylphenol (PVP) layer to the P3HT interface and alter the conductivity of the semiconducting channel.

To facilitate a production of protons at the gate electrode, the chemical reaction shown in Equation (1) was used [51]. GST was used to promote the conjugation reaction between GSH and 1-chloro-2,4-dinitrobenzene (CDNB) producing hydrochloric acid. As the Nafion film is a porous membrane, the hydrogen ions produced are able to diffuse through the film and dope the P3HT.



Firstly, the required concentrations of the reactants were calculated so that the number of protons produced would be of the similar order to that of the glucose sensors. The glucose oxidase enzyme used had a molecular weight of 160,000 g/mol and had over 100 units/mg. One unit oxidises 1  $\mu$ mole of D-glucose, with a molecular weight of 180.16 g/mol, per minute and produces two protons through the decomposition of the generated hydrogen peroxide [50]. Assuming 20 mg/ml of glucose oxidase was used and a 5  $\mu$ L drop of it is placed onto the device, this was 5  $\mu$ g of glucose oxidase, comprising of 10 units. Then, if 5  $\mu$ L of 1 mM glucose, or 5 nmoles, was placed onto the device, with a rate of reaction of 10  $\mu$ moles/min and assuming complete exposure, this would all react within 0.5 ms. As the reaction in Equation (1) only produces one hydrogen ion, twice the concentration of GSH was needed. Therefore, in a 5  $\mu$ L drop of 2 mM GSH there are 10 nanomoles. One unit of GST conjugates 1  $\mu$ mole/min and comprises of at least 25 units/mg. To obtain the same rate of proton generation 20 units or 0.8 mg would be required. This result would mean that in a 5  $\mu$ L drop the GST concentration would need to be 160 mg/mL which is far higher than practical. So, the highest concentration of GST available was used, which was 10  $\mu$ M. Therefore, it should have taken approximately 38.4 seconds for all of the GSH and CDNB to react which was still well within the time limits of the sensing measurement and so would be suitable. The GSH concentration selected was on the higher side of the clinically relevant range as intracellular GSH concentrations are around 0.5 to 10 mM, with extracellular concentrations a few orders of magnitudes lower [52].

Secondly, pH measurements were undertaken to determine that hydrogen ions were produced. 1 mL of 10  $\mu$ M GST was mixed with 5 mL of 100 mM CDNB and then every 5 minutes, 100  $\mu$ L of 100 mM GSH was injected into the solution and the pH recorded. This test was completed both in deionized water and buffer solution, and the effect of 100 mM hydrochloric acid (HCl) directly added to the



solution was included as a control. These high concentrations ensured that any reaction that occurred would produce a clear change in pH. As shown in Figure 7, all three solutions show the same trend of increasing acidity of the solution with added volume, confirming that the reaction in Equation (1) was occurring. The difference in the response between the GSH in buffer and in water was minimal, with a slightly flatter curve at high pH values due to the buffering effect which can also be seen in the HCl test. The lower final pH of the HCl measurements was due to both the lower starting pH and also due to not requiring a reaction time.

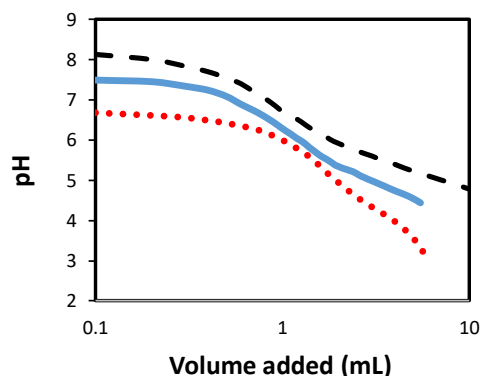


Figure 7: pH measurements showing increasing proton generation upon addition of GSH in deionised water (dashed black line) or GSH in buffer (solid blue line). For comparison, the effect of direct addition of HCl in buffer (dotted red line) is also shown.

Following confirmation that the GST-CNDB conjugation reaction produces protons as expected, the GST and CNDB were integrated into the Nafion film of the full sensor device. Initially, this integration was done by drop casting 5  $\mu\text{L}$  of each above the channel and then letting the Nafion film absorb the materials. Sensor measurements were then taken by applying  $V_{\text{DS}} = -1 \text{ V}$  and  $V_{\text{GS}} = -0.3 \text{ V}$  and after 100 seconds, the analyte was deposited on top. The normalised  $I_{\text{D}}$  responses to both the GSH and DIW are shown in Figure 8A. The current response of the GSH devices was on average approximately 3 times that of the responses to water, indicating that there was a production of HCl that was then moving through the Nafion film and doping the P3HT channel. These GSH response curves are also of similar shape to the glucose response curves presented in [2] further indicating consistency between the current modulation mechanisms between the devices. Interestingly, the current in the devices with water drops also approximately doubled which may have been due to the addition of parallel current paths through the device, reducing its resistance.

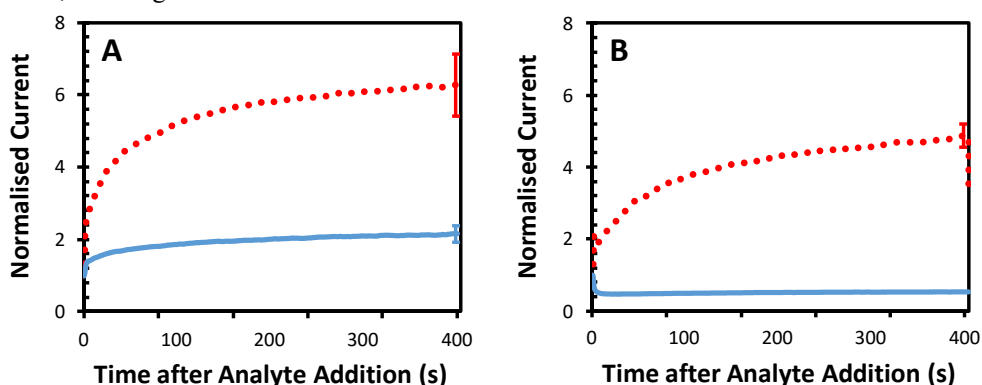


Figure 8: Peptide sensor response to de-ionised water (solid blue line) and GSH peptide solution (red dotted line) for a full sensor structure with GST and CNDB integrated into the Nafion film (A). Peptide sensor response to GSH peptide solution for a full sensor structure both with (red dotted line) and without (solid blue line) GST and CNDB integrated into the Nafion film (B). Error bars show the standard deviation of the measurement.

This response mechanism was explored further by testing the devices with and without the receptive elements, GST and CNDB (Figure 8B). The absence of any response for devices fabricated without the receptive elements indicates that the conjugation reaction does not occur and a reduced current was

observed due to de-doping of the P3HT on application of the analyte, which is consistent with processes described previously [2].

In an attempt to improve the reliability of the devices, CDNB and GST were pre-mixed so that only one drop needed to be placed on the device during fabrication. Sensor responses were then recorded and are shown in Figure 9. Firstly, similar null responses were observed for both water and GSH when the receptor was not incorporated into the device. Secondly, the observed responses with the receptor present had significant variation, with the water response slightly larger than that shown in Figure 8A, and the GSH response slightly lower. However, the GSH response was still larger than that of water, due to the generation of protons. Therefore, it is possible that the difference in film conductivity was not solely due to protonic doping but instead from an effect resulting from the integration of GST and CDNB into the device's Nafion film. It was hypothesised that the initial drops of GST and CDNB were dissolving some of the Nafion film and making it thinner above the channel region, resulting in faster ion diffusion to the P3HT interface. This observation is in accordance with the increased GSH responses observed after two separate receptor element drops (Figure 8A) compared to the lower GSH responses after only one receptor element drop in Figure 9.

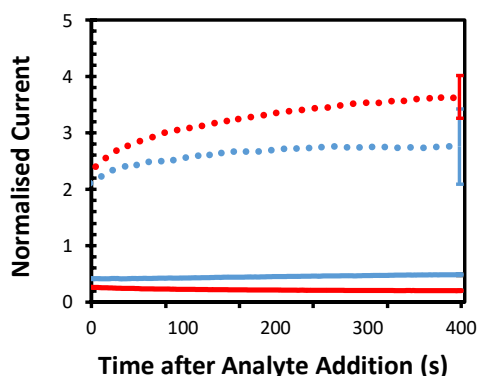


Figure 9: Peptide sensor response when premixed GST-CDNB is embedded in the Nafion film during device fabrication upon addition of GSH (red dotted line) and deionised water (blue dotted line). Also shown are the peptide sensor response for devices without premixed GST-CDNB embedded in the Nafion film following addition of GSH (solid red line) and deionised water (solid blue line). Error bars show the standard deviation of the measurement.

To test this hypothesis, GST, CDNB and either GSH or DIW were mixed together prior to dropping onto the device. This method was chosen to enable them to react and produce protons which could then be directly applied, which almost completely removes any effect of film alteration by the receptor materials. The results from this experiment are shown in Figure 10 where all devices are shown to exhibit essentially the same response. After analyte deposition, the current significantly decreased, similar to that shown in Figure 8B, when the GST and CDNB were not present. This result demonstrates that the current modulation mechanism does not occur solely due to protonic doping of the P3HT but rather due to the generation of protons at the P3HT interface.

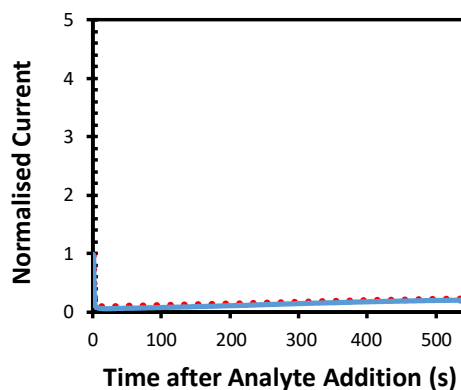


Figure 10: Peptide sensor response GST/CDNB/de-ionised water (solid blue line) and GST/CDNB/GSH peptide solution (red dotted line) for a full sensor structure. Error bars show the standard deviation of the measurement.

For the NPY detection experiments, a binding architecture based on the successful GSH-GST linkage was explored. The anti-NPY molecule that was employed includes a GST tag, thus allowing linkage with a GSH molecule. In addition, the sulphur moiety on the GSH molecule allows ready binding to a gold surface. Thus by using sequential solution adsorption of GSH, followed by anti-NPY with GST tag and finally NPY, it should be possible to obtain binding of NPY to a gold substrate and to follow the binding process using electrochemistry (Figure 11).

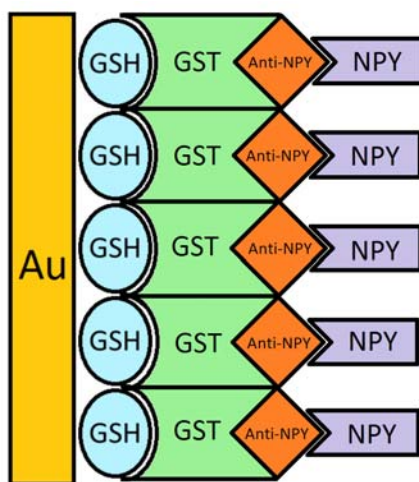


Figure 11: Schematic representation of the NPY immobilisation onto a gold substrate via binding to an anti-NPY molecule and a GSH-GST linkage.

To observe the binding of NPY and how it affects charge transfer, cyclic voltammetry measurements were taken. Firstly, a 24 ct gold wire was electrochemically polished in 1 M H<sub>2</sub>SO<sub>4</sub> by sweeping the voltage from -0.2 V to 1.6 V at a rate of 100 mV/s for 15 minutes. The wire was then rinsed with deionized water and then immersed in a 10 mM GSH solution overnight so that a self-assembled monolayer would form. This monolayer was utilised so that the GST tag on the Anti-NPY antibody could be attached and immobilised on the gold wire. The wire was immersed overnight in a 2 µg/mL anti-NPY solution. The wire was then immersed in a 100 µM NPY solution so that binding with the anti-NPY could occur. CV measurements were taken after every step using a 5 mM ferricyanide solution so the effect on charge transfer of each subsequent binding could be observed. The measurement was also performed in a Faraday cage that was constructed to minimise any external electromagnetic interference so that the low currents could be accurately measured. Figure 12A shows that for the bare gold electrode the redox peaks are clearly visible, and then after the GSH was placed on the electrode the current significantly reduced. After the anti-NPY was attached to the electrode a reduction in current is observed a further reduction in current is observed indicating that the antibody was attached to the electrode. Subsequently, a further reduction in current was observed following the NPY binding to the electrode (Figure 12B). This trend is likely to be attributed to the increase in thickness of the layer acting to more effectively block charge transfer at the gold surface. It is known that short chain thiol monolayers on gold are too thin to block ferricyanide charge transfer effectively while long alkanethiols are able to due to their well-ordered packing [53]. Also, the theoretical diffusion coefficient for nanofunctionalised electrodes has been shown to depend on the effective film thickness [54]. Therefore, by increasing the effective width of the monolayer the charge transfer should be reduced, and this corresponds to what was observed.

It is known that the typical maximum surface density of SAMs formed from alkanethiols on gold is approximately  $4.5 \times 10^{14}$  molecules/cm<sup>2</sup>. Therefore, for a surface area of approximately 1 cm<sup>2</sup>, immersed in 1 mL, the minimum concentration required for forming a dense SAM would be approximately 1 µM or  $6 \times 10^{14}$  molecules/cm<sup>3</sup> [55]. In this case, the surface area of the gold electrode was 0.636 cm<sup>2</sup>.

Therefore, the concentration of GSH was sufficient to bind to all of the sites on the electrode. Assuming a surface coverage fraction of 1, this meant that there were approximately  $2.86 \times 10^{14}$  sites for the GST to bind. This value would give a minimum concentration of 47.5 nM required for complete binding if submersed in 10mL of anti-NPY solution. The 2  $\mu\text{g/mL}$  anti-NPY solution corresponds to a concentration of approximately 60 nM, which is above the minimum threshold for complete binding. As there are two NPY binding sites per anti-NPY molecule, this means that there are  $5.73 \times 10^{14}$  sites and so a minimum concentration of 95 nM for 10mL immersion would be required. This concentration is far lower than what was used, and specifies the maximum detection limit for this particular electrode, as any additional NPY molecules would not have an available site to bind to the electrode.

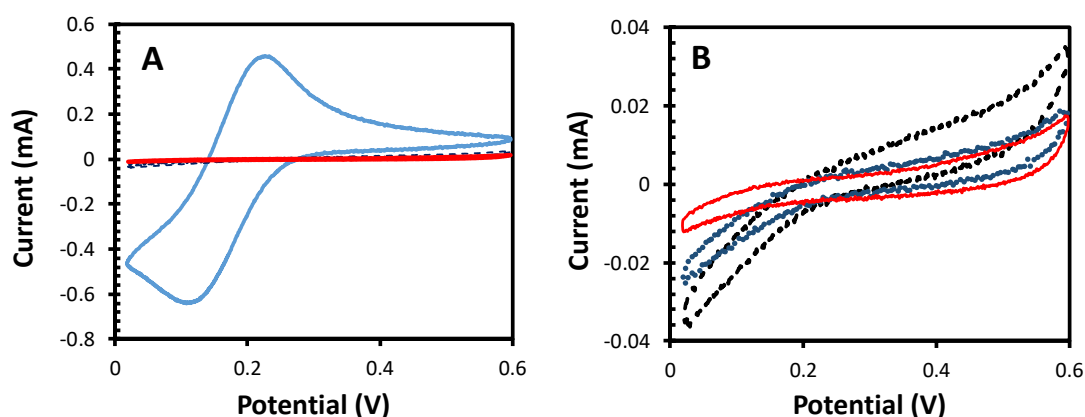


Figure 12: Electrochemical current-voltage (CV) measurement of steps involved in the immobilisation of NPY onto a gold wire electrode. A: CV measurements for bare gold wire (solid light blue line) then following immersion in: (a) GSH solution (dashed black line), (b) anti-NPY solution (blue dotted line) and (c) NPY solution (red solid line). A: Magnified CV measurements following immersion in: (a) GSH solution (dashed black line), (b) anti-NPY solution (blue dotted line) and (c) NPY solution (red solid line).

Following this experiment, the anti-NPY was integrated into a Nafion film. Nafion films were spin coated on ITO patterned substrates at 500 rpm and then 0.5 mg/mL anti-NPY was drop cast over the channel region. These were dried at 37 °C for 15 minutes until visibly dry. Sensor tests were then carried out by dropping 5  $\mu\text{L}$  of analyte, either water or 100  $\mu\text{M}$  NPY, on top of the functionalised channel region. Figure 13A shows the response of the sensor when using a bare Nafion film without any anti-NPY functionalization. When the analyte was deposited, there was a minimal change (within experimental error) in conductivity of the film, regardless of whether the analyte was NPY or water. By comparison, for a Nafion film functionalized with the anti-NPY molecule, after water was placed on the film, the current increased by almost an order of magnitude, whereas on average, the addition of an NPY drop resulted in a much smaller increase in current. Therefore, the anti-NPY being present has resulted in a film with a much higher conductivity when water was deposited, but this was nullified when NPY was placed on the device when binding occurred.

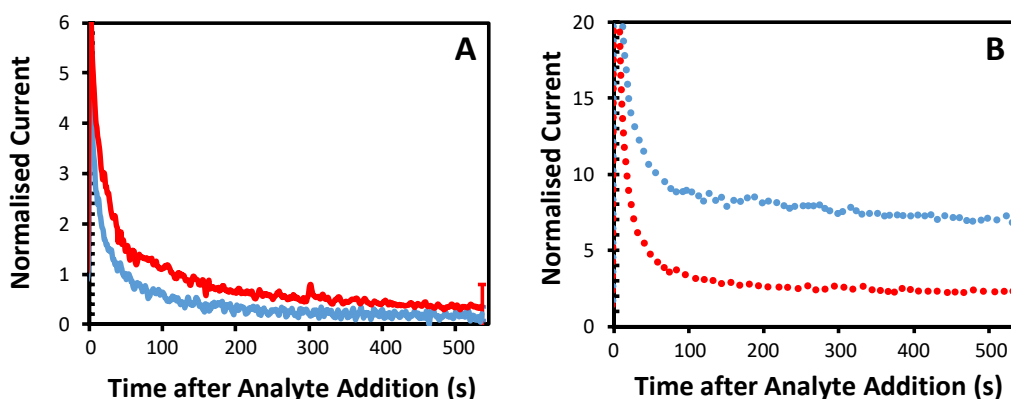


Figure 13: A. Peptide sensor response for a Nafion film without any anti-NPY added following addition of deionised water (solid blue line) and NPY solution (solid red line). B. Peptide sensor response for a Nafion film functionalised with anti-NPY following addition of deionised water (dotted blue line) and NPY solution (dotted red line). Error bars show the standard deviation of the measurement.

### Conclusions:

The detection of peptides in an organic thin film transistor architecture has been successfully demonstrated for two peptides, GSH and NPY. In both cases, by exploiting the GSH-GST linkage it has been possible to integrate the detection species (either GST alone or GST-tagged NPY antibodies) directly into the Nafion membrane gate electrode.

In the case of GSH, the GST receptor elements were incorporated into the Nafion gate electrode of an OTFT sensor device. Utilising a conjugation reaction to facilitate protonic doping of the P3HT layer, a response three times larger than that of water was obtained when 2 mM GSH was placed on the sensor, demonstrating an increase in sensitivity of five times. An investigation into the current modulation mechanism of the sensor devices revealed that the current modulation was not due to direct application of hydrogen ions to the semiconductor but due to a chemical interaction when protons were generated at the P3HT/Nafion interface. Also, it was found that the current response of the device was independent of any P3HT bleaching due to the acidity of the deposited analyte. This demonstrated that the existing sensors were much more selective than previously thought, as the sensors required the protons to be generated within the film rather than just being deposited on the surface.

Utilising monoclonal anti-NPY antibodies, electrochemical detection of NPY was also achieved, enabling detection of NPY concentrations below 95 nM. However, when anti-NPY was not in the film, the water response was three times larger, which indicated that the anti-NPY altered the conductivity of the film. This increased response was negated upon NPY binding.

### References:

1. B. Kumar, B. K. Kaushik, and Y. S. Negi, "Organic Thin Film Transistors: Structures, Models, Materials, Fabrication, and Applications: A Review," *Polymer Reviews*, vol. 54, pp. 33-111, 2014.
2. D. Elkington, M. Wasson, W. Belcher, P. C. Dastoor, and X. Zhou, "Printable organic thin film transistors for glucose detection incorporating inkjet-printing of the enzyme recognition element," *Applied Physics Letters*, vol. 106, p. 263301, 2015.
3. D. Elkington, N. Cooling, W. Belcher, P. Dastoor, and X. Zhou, "Organic Thin-Film Transistor (OTFT)-Based Sensors," *Electronics*, vol. 3, pp. 234-254, 2014.
4. M. Magliulo, M. Y. Mulla, M. Singh, E. Macchia, A. Tiwari, L. Torsi, et al., "Printable and flexible electronics: from TFTs to bioelectronic devices," *J. Mater. Chem. C*, vol. 3, pp. 12347-12363, 2015.
5. P. Atkins, *Physical Chemistry*, 6th ed. New York: W.H. Freeman and Company, 1997.
6. L. Pauling, *The Nature of the Chemical Bond*, 3 ed.: Cornell University Press, 1960.
7. J. Clark. (2004, 25 April). Introducing Amino Acids. Available: <http://www.chemguide.co.uk/organicprops/aminoacids/background.html>
8. IUPAC. *Compendium of Chemical Terminology*, 2nd ed. (the "Gold Book"). Compiled by A. D. McNaught and A. Wilkinson. Blackwell Scientific Publications, Oxford (1997). XML on-line corrected version: <http://goldbook.iupac.org> (2006-) created by M. Nic, J. Jirat, B. Kosata, and updates compiled by A. Jenkins. ISBN 0-9678550-9-8. doi:10.1351/goldbook. (25 April).
9. Zealand Pharma A/S. (25 April). What are Peptides. Available: <http://zealandpharma.com/research-and-development/key-zealand-peptide-competences/what-are-peptides>
10. P. HuiSong, "Developing a sensitive and selective method for peptide detection by mass spectrometry," Master's thesis in Proteomics and Bioinformatics, Faculty of Medicine, University of Geneva, Geneva, 2010.
11. M. A. Gillette and S. A. Carr, "Quantitative analysis of peptides and proteins in biomedicine by targeted mass spectrometry," *Nat Methods*, vol. 10, pp. 28-34, Jan 2013.
12. J. J. Pitt, "Principles and Applications of Liquid Chromatography-Mass Spectrometry in Clinical Biochemistry," *The Clinical Biochemist Reviews*, vol. 30, pp. 19-34, 2009.

13. V. H. Wysocki, K. A. Resing, Q. Zhang, and G. Cheng, "Mass spectrometry of peptides and proteins," *Methods*, vol. 35, pp. 211-22, Mar 2005.
14. S. K. G. Grebe and R. J. Singh, "Clinical peptide and protein quantification by mass spectrometry (MS)," *TrAC Trends in Analytical Chemistry*, 2016.
15. Thermo Fisher Scientific Inc. (2016, 24 October). Thermo Scientific™ Pierce™ Protein Biology. Available: <https://www.thermofisher.com/au/en/home/brands/thermo-scientific/pierce-protein-biology.html>
16. H. Wagner, W. C. Still, and C.-T. Chen, "Fluorescent, sequence-selective peptide detection by synthetic small molecules," *Science*, vol. 279, pp. 851-853, 02/06/ 1998.
17. Syed Arshad Hussain, Dibyendu Dey, Sekhar Chakraborty, Jaba Saha, Arpan Datta Roy, Santanu Chakraborty, et al., "Fluorescence Resonance Energy Transfer (FRET) sensor," *Science Letters Journal*, vol. 4, 2015.
18. B. R. White, H. M. Liljestrand, and J. A. Holcombe, "A 'turn-on' FRET peptide sensor based on the mercury binding protein MerP," *Analyst*, vol. 133, pp. 65-70, 2008.
19. L. An, Y. Tang, F. Feng, F. He, and S. Wang, "Water-soluble conjugated polymers for continuous and sensitive fluorescence assays for phosphatase and peptidase," *Journal of Materials Chemistry*, vol. 17, p. 4147, 2007.
20. H. Wang, Q. Zhang, X. Chu, T. Chen, J. Ge, and R. Yu, "Graphene oxide-peptide conjugate as an intracellular protease sensor for caspase-3 activation imaging in live cells," *Angew Chem Int Ed Engl*, vol. 50, pp. 7065-9, Jul 25 2011.
21. A. T. Timperman, K. E. Oldenburg, and J. V. Sweedler, "Native fluorescence detection and spectral differentiation of peptides containing tryptophan and tyrosine in capillary electrophoresis," *Analytical Chemistry*, vol. 67, pp. 3421-3426, 1995/10/01 1995.
22. A. K. Kenworthy, "Imaging protein-protein interactions using fluorescence resonance energy transfer microscopy," *Methods*, vol. 24, pp. 289-96, Jul 2001.
23. T. Mahmood and P.-C. Yang, "Western Blot: Technique, Theory, and Trouble Shooting," *North American Journal of Medical Sciences*, vol. 4, pp. 429-434, 2012.
24. Thermo Fisher Scientific Inc. (2016, 3 October). Overview of ELISA. Available: <https://www.thermofisher.com/au/en/home/life-science/protein-biology/protein-biology-learning-center/protein-biology-resource-library/pierce-protein-methods/overview-elisa.html>
25. A. M. Warner and S. G. Weber, "Electrochemical detection of peptides," *Analytical Chemistry*, vol. 61, pp. 2664-2668, 1989/12/01 1989.
26. J.-G. Chen, S. J. Woltman, and S. G. Weber, "Sensitivity and selectivity of the electrochemical detection of the copper(II) complexes of bioactive peptides, and comparison to model studies by rotating ring-disc electrode," *Journal of Chromatography A*, vol. 691, pp. 301-315, 2/3/ 1995.
27. L. Liu and B. Zhou, "Electrochemical Methods for Detecting  $\beta$ -Amyloid Peptides and Monitoring Their Aggregation," *International Journal of Electrochemical Science*, vol. 10, pp. 7684-7695, 2015.
28. H. P. Permentier and A. P. Bruins, "Electrochemical oxidation and cleavage of proteins with on-line mass spectrometric detection: development of an instrumental alternative to enzymatic protein digestion," *J Am Soc Mass Spectrom*, vol. 15, pp. 1707-16, Dec 2004.
29. A. Pastore, F. Piemonte, M. Locatelli, A. L. Lo Russo, L. M. Gaeta, G. Tozzi, et al., "Determination of blood total, reduced, and oxidized glutathione in pediatric subjects," *Clinical Chemistry*, vol. 47, pp. 1467-9, 2003.
30. M. Parellada, C. Moreno, K. Mac-Dowell, J. C. Leza, M. Giraldez, C. Bailón, et al., "Plasma antioxidant capacity is reduced in Asperger syndrome," *Journal of Psychiatric Research*, vol. 46, pp. 394-401.
31. N. Joseph, Y. Zhang-James, A. Perl, and S. V. Faraone, "Oxidative Stress and ADHD: A Meta-Analysis," *Journal of Attention Disorders*, vol. 19, pp. 915-924, November 1, 2015 2015.
32. B. Halliwell, "Oxidative stress and cancer: have we moved forward?," *Biochemical Journal*, vol. 401, pp. 1-11, 2007.
33. M. Valko, D. Leibfritz, J. Moncol, M. T. D. Cronin, M. Mazur, and J. Telser, "Free radicals and antioxidants in normal physiological functions and human disease," *The International Journal of Biochemistry & Cell Biology*, vol. 39, pp. 44-84, // 2007.
34. H. Hakkinen, "The gold-sulfur interface at the nanoscale," *Nat Chem*, vol. 4, pp. 443-455, 2012.
35. A. Latus, M. Enache, and E. Volanschi, "Drug-GSH interaction on GSH-Au modified electrodes: A cyclic voltammetry and electrochemical impedance spectroscopy study," *Journal of Electroanalytical Chemistry*, vol. 661, pp. 120-129, 2011.



36. J. K. Brenke, E. S. Salmina, L. Ringelstetter, S. Dornauer, M. Kuzikov, I. Rothenaigner, et al., "Identification of Small-Molecule Frequent Hitters of Glutathione S-Transferase–Glutathione Interaction," *Journal of Biomolecular Screening*, 2016.
37. R. Udomsinprasert, S. Pongjaroenkit, J. Wongsantichon, Aaron J. Oakley, L.-a. Prapanthadara, Matthew C J. Wilce, et al., "Identification, characterization and structure of a new Delta class glutathione transferase isoenzyme," *Biochemical Journal*, vol. 388, pp. 763-771, 2005.
38. L.-H. Chen, Y.-S. Choi, J. Kwon, R.-S. Wang, T. Lee, S. H. Ryu, et al., "Interaction between glutathione and glutathione-S-transferase on dendron self-assembled controlled pore glass beads," *Tetrahedron*, vol. 60, pp. 7293-7299, 2004.
39. M. Hepel and E. Tewksbury, "Ion-gating phenomena of self-assembling glutathione films on gold piezoelectrodes," *Journal of Electroanalytical Chemistry*, vol. 552, pp. 291-305, 2003.
40. K. Takehara, M. Aihara, and N. Ueda, "An ion-gate response of a glutathione monolayer assembly highly sensitive to lanthanide ions," *Electroanalysis*, vol. 6, pp. 1083-1086, 1994.
41. R. F. de Oliveira, L. Mercés, T. P. Vello, and C. C. Bof Bufon, "Water-gated phthalocyanine transistors: Operation and transduction of the peptide–enzyme interaction," *Organic Electronics*, vol. 31, pp. 217-226, 2016.
42. K. Zhang, F. Rao, J. Pablo Miramontes-Gonzalez, C. M. Hightower, B. Vaught, Y. Chen, et al., "Neuropeptide Y (NPY) Genetic Variation in the Human Promoter Alters Glucocorticoid Signaling, Yielding Increased NPY Secretion and Stress Responses," *Journal of the American College of Cardiology*, vol. 60, pp. 1678-1689, 2012.
43. *Neuropeptide Y and Related Peptides*: Springer, 2004.
44. Sigma-Aldrich. (2016, 9 October). Neuropeptide Y human. Available: <http://www.sigmaaldrich.com/catalog/product/sigma/n5017?lang=en&region=AU>
45. S. A. Monks, G. Karagianis, G. J. Howlett, and R. S. Norton, "Solution structure of human neuropeptide Y," *J Biomol NMR*, vol. 8, pp. 379-90, Dec 1996.
46. Sigma-Aldrich. (2016, 9 October). Antibody Basics. Available: <http://www.sigmaaldrich.com/technical-documents/articles/biology/antibody-basics.html>
47. P. L. Johnson, A. Molosh, S. D. Fitz, W. A. Truitt, and A. Shekhar, "Orexin, stress, and anxiety/panic states," *Prog Brain Res*, vol. 198, pp. 133-61, 2012.
48. J. Hagen, W. Lyon, Y. Chushak, M. Tomczak, R. Naik, M. Stone, et al., "Detection of orexin A neuropeptide in biological fluids using a zinc oxide field effect transistor," *ACS Chem Neurosci*, vol. 4, pp. 444-53, Mar 20 2013.
49. B. J. Sanghavi, W. Varhue, J. L. Chavez, C. F. Chou, and N. S. Swami, "Electrokinetic preconcentration and detection of neuropeptides at patterned graphene-modified electrodes in a nanochannel," *Anal Chem*, vol. 86, pp. 4120-5, May 6 2014.
50. D. Elkington, W. J. Belcher, P. C. Dastoor, and X. J. Zhou, "Detection of saliva-range glucose concentrations using organic thin-film transistors," *Applied Physics Letters*, vol. 105, 2014.
51. Sigma-Aldrich. Glutathione S-Transferase (GST) Assay Kit Technical Bulletin. Available: <https://www.sigmaaldrich.com/content/dam/sigma-aldrich/docs/Sigma/Bulletin/cs0410bul.pdf>
52. V. I. Lushchak, "Glutathione homeostasis and functions: potential targets for medical interventions," *J Amino Acids*, vol. 2012, p. 736837, 2012.
53. R. K. Mendes, R. S. Freire, C. P. Fonseca, S. Neves, and L. T. Kubota, "Characterization of self-assembled thiols monolayers on gold surface by electrochemical impedance spectroscopy," *Journal of the Brazilian Chemical Society*, vol. 15, pp. 849-855, 2004.
54. J. P. Brubaker, "A Diffusion Model for Cyclic Voltammetry with Nanostructured Electrode Surfaces," Master of Science in Chemical Engineering, School of Engineering, University of Dayton, Dayton, Ohio, 2014.
55. J. C. Love, L. A. Estroff, J. K. Kriebel, R. G. Nuzzo, and G. M. Whitesides, "Self-Assembled Monolayers of Thiolates on Metals as a Form of Nanotechnology," *Chem. Rev.*, vol. 105, pp. 1103-1169, 2005.

**List of Publications and Significant Collaborations that resulted from your AOARD supported project:** In standard format showing authors, title, journal, issue, pages, and date, for each category list the following:

**Attachments:** Publications b)